Susceptibility Mapping in Parkinson's Disease Patients at 3T

Johannes Lindemeyer[1], Ana-Maria Oros-Peusquens[1], Kathrin Reetz[1,2], and N. Jon Shah[1,2]

[1]*Institute of Neuroscience and Medicine 4, INM-4, Medical Imaging Physics, Forschungszentrum Jülich GmbH, Jülich, Germany,* [2]*Faculty of Medicine, Department of Neurology, RWTH Aachen University, JARA, Aachen, Germany*

Target Audience: Researchers with interest in phase imaging, quantitative susceptibility mapping and its applications.

Purpose: Phase imaging and, more particularly, quantitative susceptibility mapping is currently approaching clinical applications. The magnetic susceptibility of tissue is more frequently used as an indicator for the certain disease states, particularly for neurodegenerative diseases such as Parkinson's disease (PD, e.g. [1, 2]). This abstract describes a study investigating and quantifying the effect of PD on the susceptibility of brain tissue, measured with a clinical protocol at 3T. For this purpose a custom workflow for unwrapping, field map generation, background field correction and susceptibility estimation is established to optimally match the data acquired within the study.

Material and Methods:

Measurements: The measurement protocol included multiple acquisitions with a 3D gradient echo sequence using the following parameters: 192x156x128 voxel at 1mm isotropic resolution, *TR* = 51ms, α=8°, *iPAT* = 2, *BW* = 60 Hz/Px, N_{TE} = 12 echoes with *TE* = [2.58, 6.57, 10.53, 14.52, 18.48, 22.47, 26.43, 30.42, 34.38, 38.37, 42.33, 46.32] ms. Depending on the capacity of the subject to lie still for a long time, between one and three measurements with identical positioning and parameters were acquired. The study includes 30 PD patients as well as age- and gender-matched controls, of which 26 patients and 24 controls could be evaluated.

Phase Imaging Workflow: Initial brain masks, m, are estimated with *bet* [3]. Direct spatial unwrapping of the acquired echoes is not feasible due to phase pole artefacts generated by the manufacturer-provided channel recombination (*adaptive combine*). Hence, the field is estimated by unwrapping echo difference: $b_n = (1/\gamma(TE_{n+N/2} - TE_n)) \cdot \mathcal{U}(\angle\exp(\mathrm{i}\cdot(\varphi_{n+(N/2)} - \varphi_n)),\ (n \le N/2)$ and averaging the results: $b = (2/N)\cdot\sum_{n=1}^{N/2} b_n$ (where $N = N_{TE}$, γ: gyromagnetic ratio, *TE*: echo time and $\mathcal{U}$ is the spatial unwrapping operator). Unwrapping is performed with *prelude* [4]. Statistical stability and noise reduction is achieved by averaging the fieldmaps of all acquired measurements of one subject. In the averaging, global offsets have to be avoided: $b_{comb} = (1/3)\cdot\sum_{i=1}^{3} b_i - \overline{b_i(m) - b_1(m)}$. Background distortions of the resulting field maps are identified and removed by MUBAFIRE [5, 6], using standard parametrisation. Susceptibility is finally estimated in an iterative approach as described in [7] employing Tikhonov-regularised minimisation. The problem weighting matrix, *W*, and Tikhonov weighting, W_T, are set to the brain mask, *m*. Further reconstruction parameters are: regularisation coeff., λ = 0.03; 50 iterations; problem reset every 20 it.; padding with 50% of the FOV size in all dimensions.

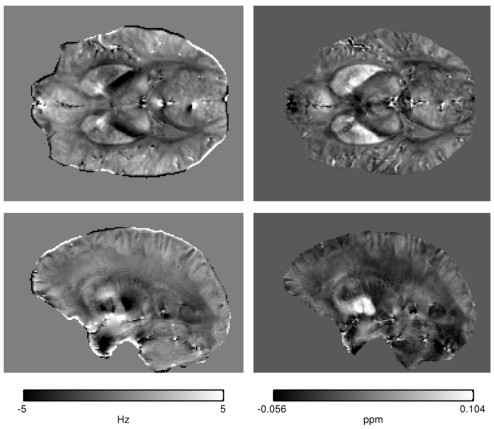

Figure 1: Transverse (upper row) and sagittal (lower row) views of background-corrected field map (left) and susceptibility (right) of a PD patient.

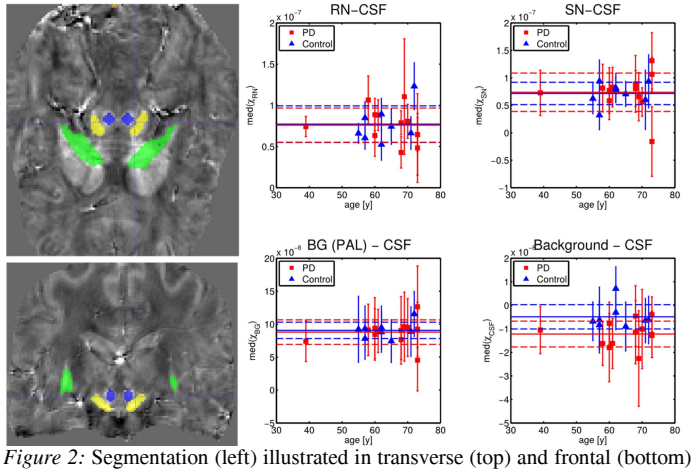

Figure 2: Segmentation (left) illustrated in transverse (top) and frontal (bottom) slice of susceptibility map. On the right hand side, correlation plots show the RN, SN, basal ganglia (BG) and CSF in relation to subject age for male subjects. The solid lines indicate the mean value and the dashed indicate standard deviation margins of all patients or controls. Age average: 64.6y for PD and 62.6 for controls.

Segmentation: Segmentation was performed to facilitate comparison between the susceptibility values of different anatomic regions. The red nuclei (RN), the substantia nigra (SN) and globus pallidus (PAL) are segmented manually based on the reconstructed susceptibility maps using ITKSnap [8]. Further, a part of the cerebrospinal fluid (CSF) is segmented to serve as a reference. The median value and the standard deviation of the susceptibility distribution inside the segmented regions are examined for age correlation and for differences between PD and controls. The complementary mask, containing the entire brain except for the segmented areas, is used to characterise global brain susceptibility.

Results: Identification and segmentation of structures in the central brain is feasible directly on susceptibility maps. The level of reconstruction-related stripe artefacts, which can affect susceptibility values for particular regions and the whole brain, is low, as assessed by visual inspection. Good-quality data from 17 PD patients (13 male and 4 female) and 17 controls (8 male and 9 female) were segmentated as illustrated in Fig. 2. Averaging of several scans/patient leads to a high SNR in the susceptibility maps; homogeneous regions such as the red nuclei (RN) have a small standard deviation. Despite the high quality of data, it was not possible to determine a change caused by disease in the susceptibility values of the iron-containing regions reported here. The mean susceptibility values for patients and controls do not reach significance level in any of the selected regions. The correlation between susceptibility and age also does not reach significance level in our data. We further reduce the group to include only male subjects (12 PD, 8 controls, 1 exclusion due to statistically insufficient segmentation volume). Interestingly, for this group the average background susceptibility shows clearly decreased susceptibility values with a difference of about -0.07ppm between healthy and diseased state (Fig. 2), the standard deviation of each average being +/- 0.05ppm. The 'background' value reflects the average susceptibility of the majority of brain tissue.

Discussion and Conclusions: The study demonstrates the feasibility of susceptibility mapping in PD in a clinical setting. Whereas iron metabolism is supposed to play an important role in PD, quantitative susceptibility mapping did not reveal clear changes in the susceptibility of particular regions known to be affected by PD. However, on a global level, the susceptibility difference between the whole brain and CSF was significantly larger (in absolute value) in male PD patients. This might be due to changes in the susceptibility of CSF in PD, or to global changes in the susceptibility of the brain tissue in PD, or both. If we assign susceptibility changes to changes in iron deposits only, the susceptibility values indicate a decrease in iron content in the whole brain (and/or increase in CSF iron levels), with a slightly reduced decrease in regions that show high iron content in the healthy state. Indeed, systemic changes affect the levels of ferritin and transferrin in PD [9] and might lead to decreased brain ferritin content, and the level of ferritin in CSF was found to be slightly (but not significantly) increased in PD [10]. Global brain susceptibility changes in PD are reported here for the first time, to our knowledge. In the future, measurements at higher field strength with higher phase SNR and the use of an appropriate reference for susceptibility values will help to clarify this observation.

References: [1] Schäfer et al. *Hum brain Mapp*, vol. 33, pp. 2831–42, Dec. 2012. [2] A. K. Lotfipour et al. *JMRI*, vol. 35, pp. 48–55, Jan. 2012. [3] M. Jenkinson et al. *Medical Image Analysis*, vol. 5, no. 2, pp. 143–156, 2001. [4] M. Jenkinson. Fast, automated, N-dimensional phase-unwrapping algorithm. *MRM*, vol. 49, pp. 193–7, Jan. 2003. [5] J. Lindemeyer et al. *Annual Meeting of the European Society for Magnetic Resonance in Medicine and Biology*, p. 507, 2011. [6] J. Lindemeyer et al. *Proc. Int. Soc. Mag. Reson. Med.*, vol. 20, p. 2329, 2012. [7] L. de Rochefort et al. *MRM*, vol. 63, pp. 194–206, Jan. 2010. [8] P. A. Yushkevich et al. *Neuroimage*, vol. 31, no. 3, pp. 1116–1128, 2006.; [9] Logroscino et al., Neurology 1997; [10] Kuiper et al, J.Neural Transm 1994.